Electronic Supplementary Material (ESI) for Chemical Science.

Supporting information

Carboxylate ester-based electrolytes for Na-ion batteries

Yunan Qin [a], Seong-Gyu Choi [a], Lucia Mason [a], Jing Liu [a], Zongjian Li [a], Tao Gao [a]*

[a] Department of Chemical Engineering, University of Utah, Salt Lake City, Utah, USA 84114

*Email: taogao@chemeng.utah.edu

Table S1. Summary of common solvents used in SIBs.

Classification	Typical electrolyte	Ref.
Carbonate	1M $NaPF_6$-PC-0.5% FEC	1
	5m NaFSI-NaFTI-NaOTf-PC	2
	1M $NaClO_4$-EC/PC	3
	1M $NaClO_4$-EC/DMC	4
	0.5 M $NaClO_4$-EC/PC/DEC	5
Ether	1M $NaPF_6$-diglyme	6
	NaFSI/DME	7
	0.5M $NaBPh_4$-DME	8
	0.9 M $NaPF_6$-0.1 M $NaBF_4$-diglyme	9
	1 M $NaPF_6$-THF	10
Phosphate	1:3 $NaClO_4$-TMP-5 vol % FEC	11
	NaFSI:TEP=1:1.5	12
	0.16-0.85 M NaFSI-TEP/$PhCF_3$	13
	NaFSI-TEP/TTE (1:1.5:2 in molar ratio)	14
Fluorinated	1.5 M NaFSI DMC-TFP	15
	0.9M NaFSI-TFEP	16
	1M $NaClO_4$-FEC	17
Sulfolane	1M $NaClO_4$-EC/PC/SL	18
Nitrile	50 mol % NaFSI/SN	19

Table S2. Electrolytes and their low-temperature electrochemical performances in SIBs. ("NA" stands for "not available".)

Electrolyte	Electrode	LT (℃)	Capacity at RT (mAh/g)	Capacity retention at LT	Retention capacity/ number of cycles at LT	Voltage	Ref.
0.8M $NaPF_6$-PC/EMC-2wt%FEC	$NaNi_{1/3}Fe_{1/3}Mn_{1/3}O_2$ // hard carbon	1	750 mAh@1C	~48%@1C	80%@1C/2500	1.5-3.8	20
1 M $NaPF_6$ in EC-PC-DMC-20%MA	NVPF // hard carbon	0	~95@0.2C	~84%@0.2C	NA	2-4.3	21
1 M $NaPF_6$-EC/PC-5wt%FEC	$Na_{0.67}Ni_{0.1}Co_{0.1}Mn_{0.8}O_2$ // hard carbon	-20	178.5@0.2C	79.8%@0.2C	68.2@0.5C /100	1.4-4.1	22
1 M $NaClO_4$-PC-2 vol% FEC	$Na_{0.8}Ni_{0.4}Ti_{0.6}O_2$ // $NaV_{1.25}Ti_{0.75}O_4$	-20	97@0.2C	95.9%@0.2C	17%@5 C /10	0.5-4	23
1 M $NaClO_4$-EC/PC	$Na_{3.5}V_2(PO_4)_2F_3$ // hard carbon	-20	306@NA	80.4%@NA	~27.3%@ NA/5	1.6-4.3	24
1 M $NaClO_4$-EC/PC-5wt%FEC	Se@graphene // NVPOF	-25	128.1@ 0.02 $A\cdot g^{-1}$	60.7%@0.04$A\cdot g^{-1}$	75%@0.4A g^{-1}/1000	1.2-4.3	25
1M $NaClO_4$-EC/PC	$Na_3V_2(PO_4)_2O_2F$ // FeS@C	-25	484@0.01 $A\cdot g^{-1}$	30.5@0.1$A\cdot g^{-1}$	>66.7@0.1$A\cdot g^{-1}$/30	1.2-4.2	26
1 M $NaPF_6$-diglyme	Bi // NFPP@C	-70	305@0.33C	70.19%@0.03C	NA	1-3.5	27

Table S3. Temperature influence on bulk and interfacial performance of SIBs and SMBs using different electrolytes. ("NA" stands for "not available".)

Classification	Electrolyte	Electrode	LT (°C)	Conductivity at RT (mS/cm)	Rate of conductivity increase (mS/cm/°C)	Rate of R_{int} decrease (Ω/°C)	Rate of R_{ct} decrease (Ω/°C)	Ref.
Carbonate	1.0 M $NaPF_6$-EC/EMC	Na / $Na_3V_2(PO_4)_3$	-20	7.1	0.13	NA	NA	28
	1.0 M NaTFSI-FEC/FEMC			~4	0.07	NA	NA	
	1.0 M NaTFSI-FEC/FEMC/FB			~3.5	0.04	NA	NA	
	1 M $NaClO_4$-PC-2 vol% FEC	Na / $NaV_{1.25}Ti_{0.75}O_4$	-20	NA	NA	210.36	193.47	23
		Na / hard carbon	-20	NA	NA	473.49	239.46	
	1 M $NaPF_6$-EC/PC/DMC	$Na_3V_2(PO_4)_2F_3$ / hard carbon	-10	13.7	0.19	0.42	1.76	21
	1 M $NaPF_6$-EC/PC/DMC/MA			11.7	0.20	NA	NA	
	0.8 M $NaPF_6$-FEC/EMC/HFE	Na / $Na_3V_2(PO_4)_2O_2F$	-40	6.0	0.07	NA	NA	29
	1 M $NaClO_4$-EC/PC	$Na_3V_2(PO_4)_2F_3$ / hard carbon	-20	NA	NA	1.32	25.56	24
	0.5 M $NaPF_6$-EC/PC	Na / $Na_3V_2(PO_4)_2F_3$	-20	6.2	0.09	0.34	164.76	30
	0.5 M $NaPF_6$-diglyme			4.1	0.04	0.17	0.25	
Ether	0.3 M $NaPF_6$-diglyme /THF	Na / $Na_3V_2(PO_4)_3$	-20	~3.6	0.03	NA	NA	31
	0.8 M NaOTf-THF/DME	Na / $NaTi_2(PO_4)_3$	-60	~1.5	0.01	NA	NA	32
	0.5M NaOTf-diglyme /DOL	Na@Mxene / $Na_3V_2(PO_4)_3$	-40	3.7	0.06	NA	NA	33
	0.8 M NaOTf-0.2 M $NaBF_4$-diglyme	Na / $Na_3V_2(PO_4)_3$	-40	~3.2	0.04	NA	NA	34

Table S4. Physical properties of carboxylate esters and carbonate esters. ("NA" stands for "not available".)

Carbon atom	Group	Solvent	Abbreviation	Formula	MW (g/mol)	Boiling point (℃)	Melting point (℃)	Flash point (℃)	Viscosity (cP)	Dielectric constant	Dipole moment (D)	Donor numbers (kcal/mol)	Ref.
3	carboxylate	methyl acetate	MA	$C_3H_6O_2$	74	57	-98	-13	0.36	7.07	1.69	16.5	35,36
	carbonate	dimethyl carbonate	DMC	$C_3H_6O_3$	90	91	5	18	0.59	3.09	0.91	17.2	35,36,37
4	carboxylate	ethyl acetate	EA	$C_4H_8O_2$	88	77	-84	-3	0.42	5.99	1.88	17.1	36,38,39
		methyl propionate	MP	$C_4H_8O_2$	88	80	-88	-2	0.43	6.20	1.73	11	39,40
	carbonate	ethyl methyl carbonate	EMC	$C_4H_8O_3$	104	108	-15	23	0.65	2.90	NA	6.5	35,37,40
5	carboxylate	n-propyl acetate	NPA	$C_5H_{10}O_2$	102	102	-95	14	0.55	6.30	1.79	16	40
		i-propyl acetate	IPA	$C_5H_{10}O_2$	102	89	-73	4	0.49	NA	1.75	17.5	40
		ethyl propionate	EP	$C_5H_{10}O_2$	102	99	-73	12	0.49	5.70	1.74	17.1	41
		methyl Butyrate	MB	$C_5H_{10}O_2$	102	102	-95	11	0.60	5.60	1.72	NA	40
		methyl isobutyrate	MIB	$C_5H_{10}O_2$	102	91	-85	3	0.69	NA	NA	NA	42
	carbonate	diethyl carbonate	DEC	$C_5H_{10}O_3$	118	126	-43	25	0.75	2.81	1.07	16	37,40

Table S5. Conductivity and electrochemical performance (HC/Na cell, 0.1C, 30 cycles) of electrolyte using 3 m NaFSI-linear carboxylate esters with different chain lengths. ("NA" stands for "not available".)

Carbon atom	Solvent	Conductivity (mS/cm)	Capacity (mAh/g)	ICE (%)	Average CE (%)
3	MA	14.13	176	50.03	99.52
4	EA	11.31	63	32.7	99.1
	MP	10.27	44	25.28	98.75
5	NPA	7.39	40	24.44	94.34
	IPA	6.00	0	58.33	NA
	EP	6.06	43	17.58	92.04
	MB	6.06	22	23.53	NA
	MIB	7.38	34	20.46	NA

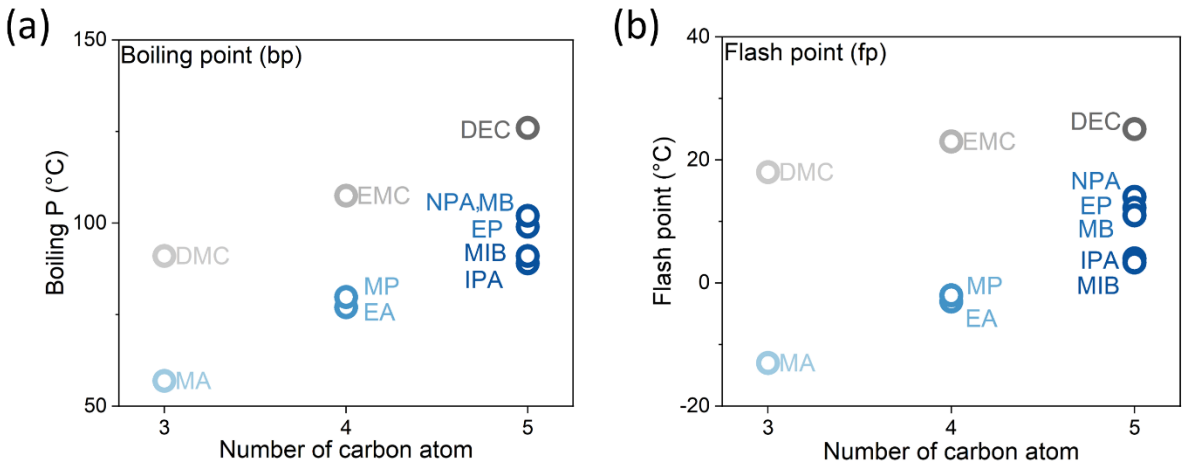

Figure S1. **Physical properties**. (a) boiling point and (b) flash point of carboxylate and carbonate solvent.

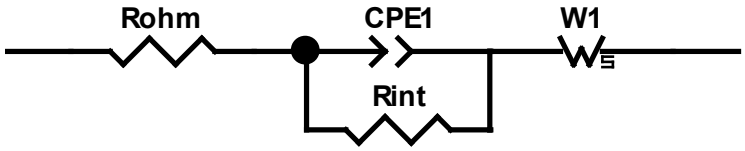

Figure S2. the equivalent circuit used for EIS fitting. R_{ohm} refers to bulk resistance, and R_{int} refers to interfacial resistance.

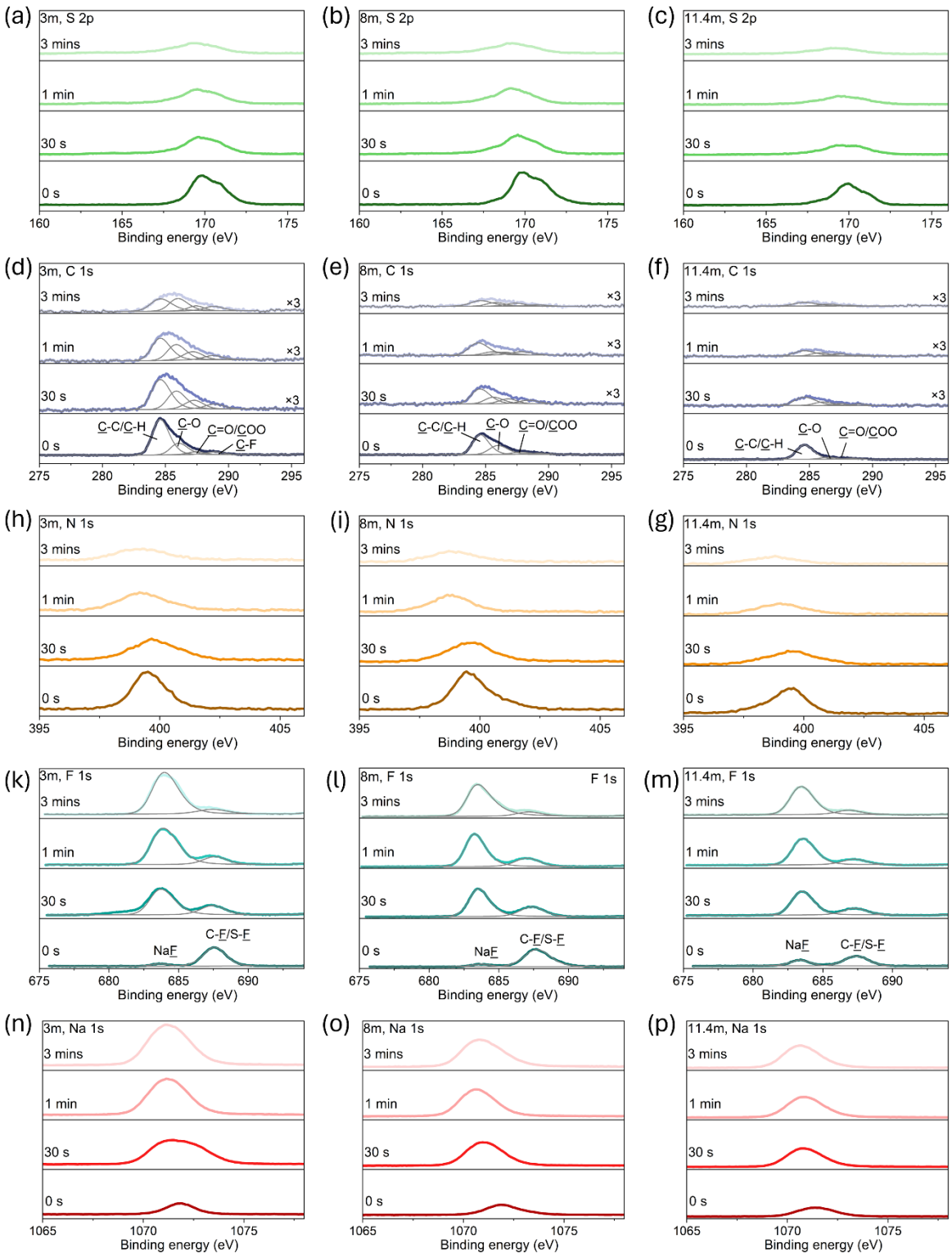

Figure S3. XPS characterization of the SEI components on cycled hard carbon anodes. (a-c) S 2p, (d-f) C 1s, (h-g) N 1s, (k-m) F 1s and (n-p) Na 1s of the hard carbon anodes after 30 cycles in 3 m NaFSI-MA (a, d, h, k, n), 8 m NaFSI-MA (b, e, i, l, o) and 11.4 m NaFSI-MA (c, f, g, m, p).

Solvation number calculation. The coordinated and uncoordinated solvent have been deconvoluted according to reported method[43]. The area of absorption is assumed to be proportional to the amount of coordinated and uncoordinated solvent. The relative areas of coordinated and uncoordinated solvent are used to estimate the concentration of solvent molecules coordinated to the Na^+ cation using Equation 1, where C_{CO}, C^0, and C_{Na} are the concentrations of coordinated solvent, total solvent, and sodium salt, respectively, N is the average solvation number, and A_{CO} and A_{UC} are relative areas of the FT-IR bands for coordinated carbonate and uncoordinated solvent, respectively.

$$C_{co} = NC_{Na}$$

$$C_{co} = \frac{A_{co}}{A_{co} + A_{UC}} C^0$$

$$N = \frac{A_{co}}{A_{co} + A_{UC}} \frac{C^0}{C_{Na}} \qquad (1)$$

The absorbance bands around 1750cm^{-1} are characteristics of C=O groups in DMC[44].

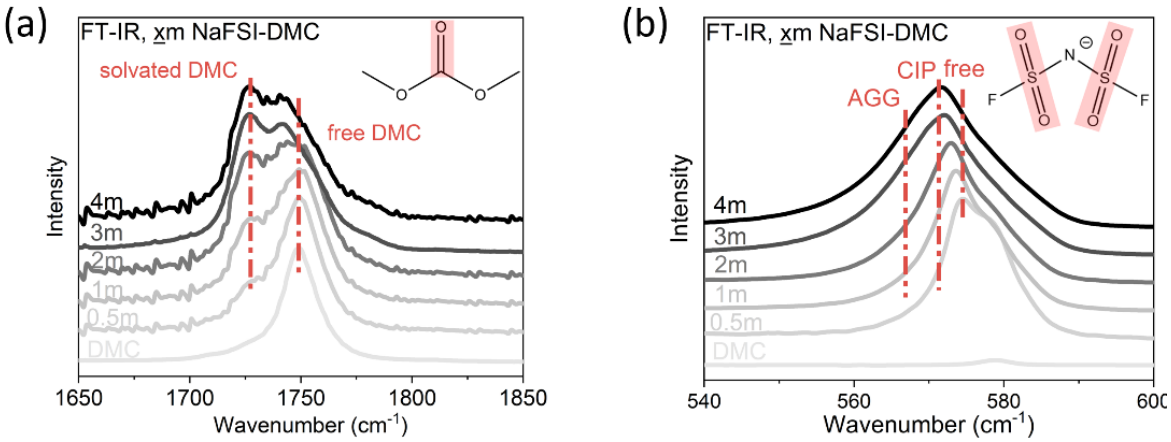

Figure S4. (a,b) FT-IR profiles of NaFSI-DMC with different salt concentration. (x = 0.5, 1, 2, 3, 4)

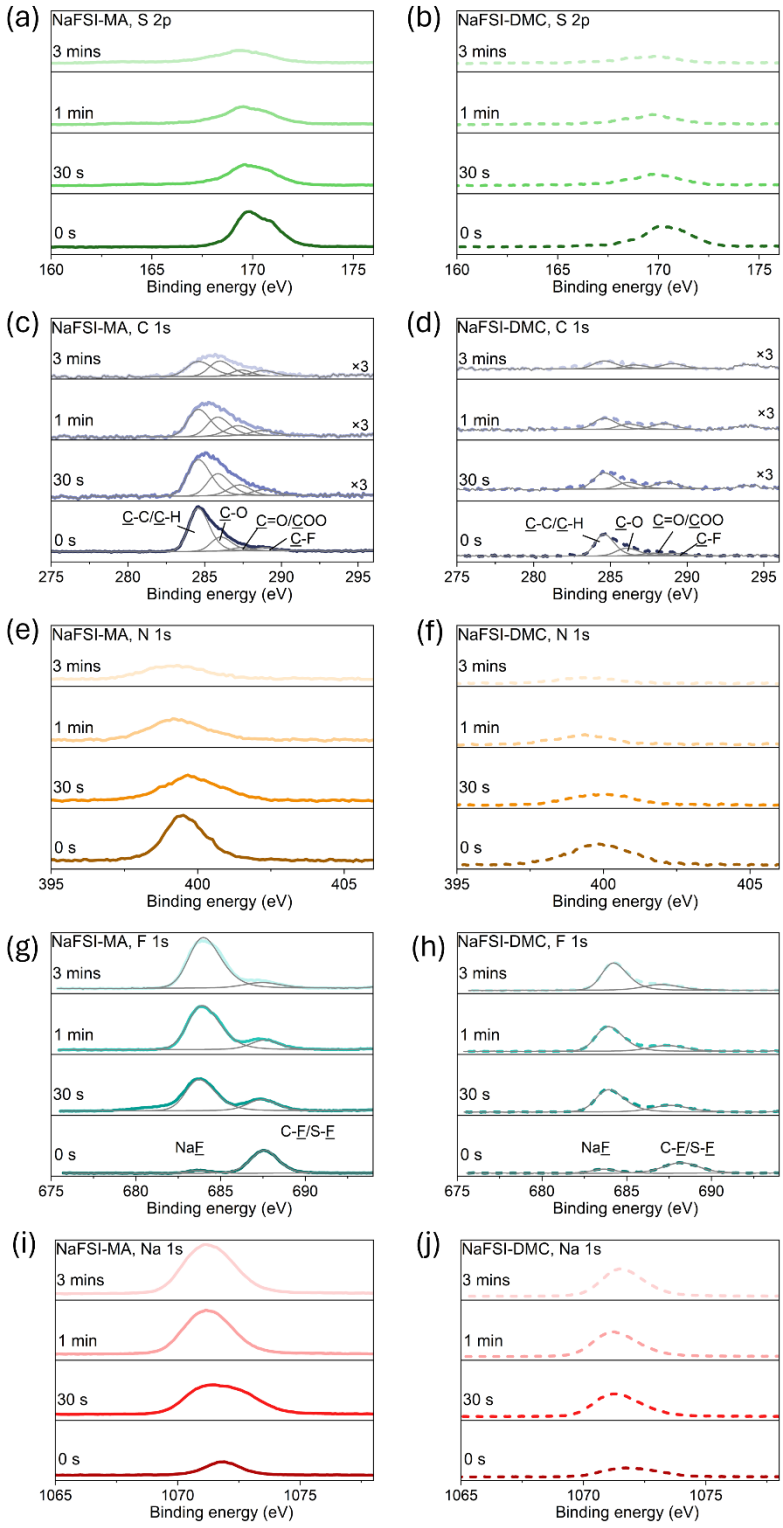

Figure S5. XPS characterization of the SEI components on cycled hard carbon anodes. (a, b) Na 1s, (c, d) N 1s, (e, f) S 2p, (g, h) C 1s and (i, j) F 1s of the hard carbon anodes after 30 cycles in NaFSI-MA (a, c, e, g, i) and NaFSI-DMC (b, d, f, h, j).

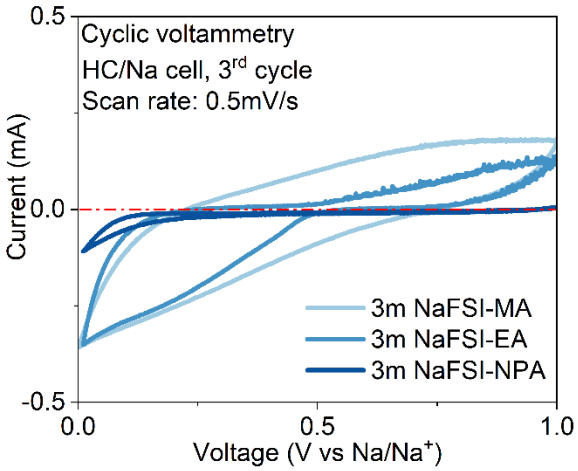

Figure S6. CV curves of HC/Na cell using 3 m carboxylate ester-based electrolytes.

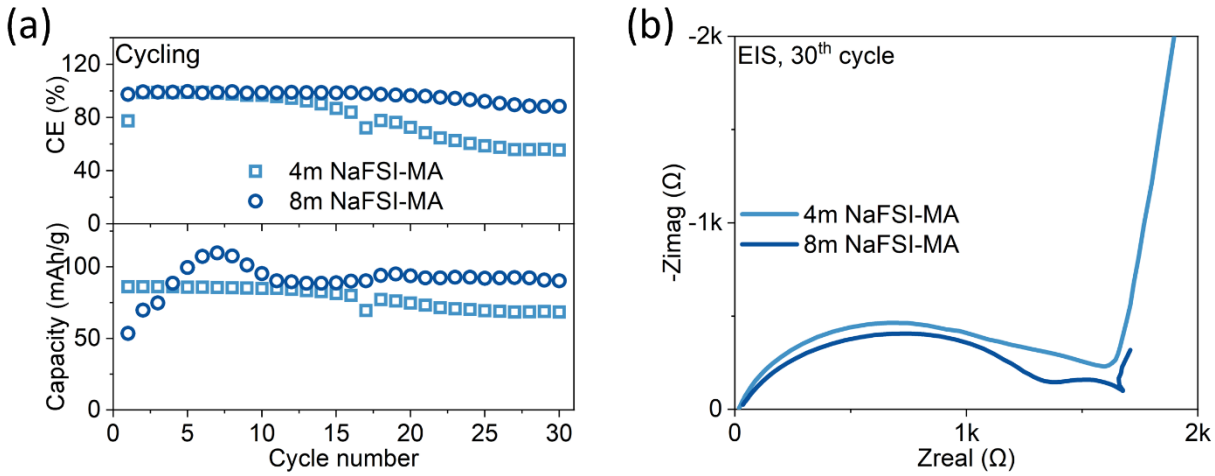

Figure S7. (a) Cycling performance (top: CE; bottom: capacity) and (b) EIS curve of NVP/Na cell using 4 m and 8m NaFSI-MA electrolytes.

Reference

(1) Dahbi, M.; Nakano, T.; Yabuuchi, N.; Fujimura, S.; Chihara, K.; Kubota, K.; Son, J. Y.; Cui, Y. T.; Oji, H.; Komaba, S. Effect of Hexafluorophosphate and Fluoroethylene Carbonate on Electrochemical Performance and the Surface Layer of Hard Carbon for Sodium-Ion Batteries. *ChemElectroChem* **2016**, *3* (11), 1856–1867. https://doi.org/10.1002/celc.201600365.

(2) Hwang, J.; Sivasengaran, A. N.; Yang, H.; Yamamoto, H.; Takeuchi, T.; Matsumoto, K.; Hagiwara, R. Improvement of Electrochemical Stability Using the Eutectic Composition of a Ternary Molten Salt System for Highly Concentrated Electrolytes for Na-Ion Batteries. *ACS Appl. Mater. Interfaces* **2021**, *13* (2), 2538–2546. https://doi.org/10.1021/acsami.0c17807.

(3) Ponrouch, A.; Marchante, E.; Courty, M.; Tarascon, J. M.; Palacín, M. R. In Search of an Optimized Electrolyte for Na-Ion Batteries. *Energy Environ. Sci.* **2012**, *5* (9), 8572–8583. https://doi.org/10.1039/c2ee22258b.

(4) Barker, J.; Saidi, M. Y.; Swoyer, J. L. A Sodium-Ion Cell Based on the Fluorophosphate Compound NaVPO4F. *Electrochem. Solid-State Lett.* **2003**, *6* (1). https://doi.org/10.1149/1.1523691.

(5) Lee, Y.; Lee, J.; Kim, H.; Kang, K.; Choi, N. Highly Stable Linear Carbonate-Containing Electrolytes with Fl Uoroethylene Carbonate for High-Performance Cathodes in Sodium-Ion Batteries. *J. Power Sources* **2016**, *320*, 49–58. https://doi.org/10.1016/j.jpowsour.2016.04.070.

(6) Westman, K.; Dugas, R.; Jankowski, P.; Wieczorek, W.; Gachot, G.; Morcrette, M.; Irisarri, E.; Ponrouch, A.; Palac, M. R.; Tarascon, J.; Johansson, P. Diglyme Based Electrolytes for Sodium-Ion Batteries. *ACS Appl. Energy Mater.* **2018**, *1*, 2671–2680. https://doi.org/10.1021/acsaem.8b00360.

(7) Schafzahl, L.; Hanzu, I.; Wilkening, M.; Freunberger, S. A. An Electrolyte for Reversible Cycling of Sodium Metal and Intercalation Compounds. *ChemSusChem* **2017**, *10* (2), 401–408. https://doi.org/10.1002/cssc.201601222.

(8) Morikawa, Y.; Yamada, Y.; Doi, K.; Nishimura, S. I.; Yamada, A. Reversible and High-Rate Hard Carbon Negative Electrodes in a Fluorine-Free Sodium-Salt Electrolyte. *Electrochemistry* **2020**, *88* (3), 151–156. https://doi.org/10.5796/electrochemistry.19-00073.

(9) Li, Y.; Zhou, Q.; Weng, S.; Ding, F.; Qi, X.; Lu, J.; Li, Y.; Zhang, X.; Rong, X.; Lu, Y.; Wang, X.; Xiao, R.; Li, H.; Huang, X.; Chen, L.; Hu, Y. S. Interfacial Engineering to Achieve an Energy Density of over 200 Wh Kg−1 in Sodium Batteries. *Nat. Energy* **2022**, *7* (6), 511–519. https://doi.org/10.1038/s41560-022-01033-6.

(10) Tang, Z.; Wang, H.; Wu, P.; Zhou, S.; Huang, Y.; Zhang, R.; Sun, D.; Tang, Y.; Wang, H. Electrode–Electrolyte Interfacial Chemistry Modulation for Ultra-High Rate Sodium-Ion Batteries. *Angew. Chemie Int. Ed.* **2022**, *61* (18). https://doi.org/10.1002/anie.202200475.

(11) Liu, X.; Jiang, X.; Zeng, Z.; Ai, X.; Yang, H.; Zhong, F.; Xia, Y.; Cao, Y. High Capacity

and Cycle-Stable Hard Carbon Anode for Nonflammable Sodium-Ion Batteries. *ACS Appl. Mater. Interfaces* **2018**, *10* (44), 38141–38150. https://doi.org/10.1021/acsami.8b16129.

(12) Jin, Y.; Xu, Y.; Xiao, B.; Engelhard, M. H.; Yi, R.; Vo, T. D.; Matthews, B. E.; Li, X.; Wang, C.; Le, P. M. L.; Zhang, J. G. Stabilizing Interfacial Reactions for Stable Cycling of High-Voltage Sodium Batteries. *Adv. Funct. Mater.* **2022**, *2204995*. https://doi.org/10.1002/adfm.202204995.

(13) Chen, B.; Yang, X.; Liu, Y.; Dai, S.; Qi, X.; Hu, Y.; Pan, H. Solvent Reorganization and Additives Synergistically Enable High-Performance Na- Ion Batteries. **2023**. https://doi.org/10.1021/acsenergylett.2c02353.

(14) Jin, Y.; Xu, Y.; Le, P. M. L.; Vo, T. D.; Zhou, Q.; Qi, X.; Engelhard, M. H.; Matthews, B. E.; Jia, H.; Nie, Z.; Niu, C.; Wang, C.; Hu, Y.; Pan, H.; Zhang, J. G. Highly Reversible Sodium Ion Batteries Enabled by Stable Electrolyte-Electrode Interphases. *ACS Energy Lett.* **2020**, *5* (10), 3212–3220. https://doi.org/10.1021/acsenergylett.0c01712.

(15) Jin, Y.; Le, P. M. L.; Gao, P.; Xu, Y.; Xiao, B.; Engelhard, M. H.; Cao, X.; Vo, T. D.; Hu, J.; Zhong, L.; Matthews, B. E.; Yi, R.; Wang, C.; Li, X.; Liu, J.; Zhang, J. G. Low-Solvation Electrolytes for High-Voltage Sodium-Ion Batteries. *Nat. Energy* **2022**, *7* (8), 718–725. https://doi.org/10.1038/s41560-022-01055-0.

(16) Jiang, X.; Liu, X.; Zeng, Z.; Xiao, L.; Ai, X.; Yang, H.; Cao, Y. A Bifunctional Fluorophosphate Electrolyte for Safer Sodium-Ion Batteries. *iScience* **2018**, *10*, 114–122. https://doi.org/10.1016/j.isci.2018.11.020.

(17) Wu, S.; Su, B.; Ni, K.; Pan, F.; Wang, C.; Zhang, K.; Yu, D. Y. W.; Zhu, Y.; Zhang, W. Fluorinated Carbonate Electrolyte with Superior Oxidative Stability Enables Long-Term Cycle Stability of Na2/3Ni1/3Mn2/3O2 Cathodes in Sodium-Ion Batteries. *Adv. Energy Mater.* **2021**, *11* (9), 1–8. https://doi.org/10.1002/aenm.202002737.

(18) Vo, D. T.; Phan, A. L. B.; Tran, T. B.; Nguyen, V. H.; Le, T. M. L.; Garg, A.; Okada, S.; Le, P. M. L. Physicochemical and Electrochemical Properties of Sulfolane – Carbonate Electrolytes for Sodium-Ion Conduction. *J. Mol. Liq.* **2020**, *307*. https://doi.org/10.1016/j.molliq.2020.112982.

(19) Takada, K.; Yamada, Y.; Watanabe, E.; Wang, J.; Sodeyama, K.; Tateyama, Y.; Hirata, K.; Kawase, T.; Yamada, A. Unusual Passivation Ability of Superconcentrated Electrolytes toward Hard Carbon Negative Electrodes in Sodium-Ion Batteries. *ACS Appl. Mater. Interfaces* **2017**, *9* (39), 33802–33809. https://doi.org/10.1021/acsami.7b08414.

(20) Che, H.; Yang, X.; Yu, Y.; Pan, C.; Wang, H.; Deng, Y.; Li, L.; Ma, Z. F. Engineering Optimization Approach of Nonaqueous Electrolyte for Sodium Ion Battery with Long Cycle Life and Safety. *Green Energy Environ.* **2021**, *6* (2), 212–219. https://doi.org/10.1016/j.gee.2020.04.007.

(21) Desai, P.; Abou-Rjeily, J.; Tarascon, J. M.; Mariyappan, S. Practicality of Methyl Acetate as a Co-Solvent for Fast Charging Na-Ion Battery Electrolytes. *Electrochim. Acta* **2022**, *416* (March), 140217. https://doi.org/10.1016/j.electacta.2022.140217.

(22) Li, Y.; Zhao, Y.; Feng, X.; Wang, X.; Shi, Q.; Wang, J.; Wang, J.; Zhang, J.; Hou, Y. A

Durable P2-Type Layered Oxide Cathode with Superior Low-Temperature Performance for Sodium-Ion Batteries. *Sci. China Mater.* **2022**, *65* (2), 328–336. https://doi.org/10.1007/s40843-021-1742-8.

(23) Li, Q.; Jiang, K.; Li, X.; Qiao, Y.; Zhang, X.; He, P.; Guo, S.; Zhou, H. A High-Crystalline NaV1.25Ti0.75O4 Anode for Wide-Temperature Sodium-Ion Battery. *Adv. Energy Mater.* **2018**, *8* (25), 1–7. https://doi.org/10.1002/aenm.201801162.

(24) Lin, X.; Du, X.; Tsui, P. S.; Huang, J. Q.; Tan, H.; Zhang, B. Exploring Room- and Low-Temperature Performance of Hard Carbon Material in Half and Full Na-Ion Batteries. *Electrochim. Acta* **2019**, *316*, 60–68. https://doi.org/10.1016/j.electacta.2019.05.106.

(25) Wang, Y.; Hou, B.; Guo, J.; Ning, Q.; Pang, W.; Wang, J. An Ultralong Lifespan and Low-Temperature Workable Sodium-Ion Full Battery for Stationary Energy Storage. **2018**, *1703252*, 1–8. https://doi.org/10.1002/aenm.201703252.

(26) Fan, H. H.; Li, H. H.; Guo, J. Z.; Zheng, Y. P.; Huang, K. C.; Fan, C. Y.; Sun, H. Z.; Li, X. F.; Wu, X. L.; Zhang, J. P. Target Construction of Ultrathin Graphitic Carbon Encapsulated FeS Hierarchical Microspheres Featuring Superior Low-Temperature Lithium/Sodium Storage Properties. *J. Mater. Chem. A* **2018**, *6* (17), 7997–8005. https://doi.org/10.1039/c8ta01392f.

(27) Li, Z.; Zhang, Y.; Zhang, J.; Cao, Y.; Chen, J.; Liu, H.; Wang, Y. Sodium-Ion Battery with a Wide Operation-Temperature Range from −70 to 100 °C. *Angew. Chemie* **2022**, *134* (13). https://doi.org/10.1002/ange.202116930.

(28) Liu, X.; Zheng, X.; Qin, X.; Deng, Y.; Dai, Y.; Zhao, T.; Wang, Z.; Yang, H.; Luo, W. Temperature-Responsive Solid-Electrolyte-Interphase Enabling Stable Sodium Metal Batteries in a Wide Temperature Range. *Nano Energy* **2022**, *103* (PA), 107746. https://doi.org/10.1016/j.nanoen.2022.107746.

(29) Zheng, X.; Gu, Z.; Fu, J.; Wang, H.; Ye, X.; Huang, L.; Liu, X.; Wu, X.; Luo, W.; Huang, Y. Knocking down the Kinetic Barriers towards Fast-Charging and Low-Temperature Sodium Metal Batteries. *Energy Environ. Sci.* **2021**, *14* (9), 4936–4947. https://doi.org/10.1039/d1ee01404h.

(30) Zheng, Y. Q.; Sun, M. Y.; Yu, F. Da; Deng, L.; Xia, Y.; Jiang, Y. S.; Que, L. F.; Zhao, L.; Wang, Z. B. Utilizing Weakly-Solvated Diglyme-Based Electrolyte to Achieve a 10,000-Cycles Durable Na3V2(PO4)2F3 Cathode Endured at − 20 °C. *Nano Energy* **2022**, *102* (August). https://doi.org/10.1016/j.nanoen.2022.107693.

(31) Wang, Z.; Zheng, X.; Liu, X.; Huang, Y.; Huang, L.; Chen, Y.; Han, M.; Luo, W. Promoting Fast Na Ion Transport at Low Temperatures for Sodium Metal Batteries. *ACS Appl. Mater. Interfaces* **2022**. https://doi.org/10.1021/acsami.2c10915.

(32) Zhou, J.; Wang, Y.; Wang, J.; Liu, Y.; Li, Y.; Cheng, L.; Ding, Y.; Dong, S.; Zhu, Q.; Tang, M.; Wang, Y.; Bi, Y.; Sun, R.; Wang, Z.; Wang, H. Low-Temperature and High-Rate Sodium Metal Batteries Enabled by Electrolyte Chemistry. *Energy Storage Mater.* **2022**, *50* (April), 47–54. https://doi.org/10.1016/j.ensm.2022.05.005.

(33) Wang, C.; Thenuwara, A. C.; Luo, J.; Shetty, P. P.; McDowell, M. T.; Zhu, H.; Posada-

Pérez, S.; Xiong, H.; Hautier, G.; Li, W. Extending the Low-Temperature Operation of Sodium Metal Batteries Combining Linear and Cyclic Ether-Based Electrolyte Solutions. *Nat. Commun.* **2022**, *13* (1), 1–11. https://doi.org/10.1038/s41467-022-32606-4.

(34) Thenuwara, A. C.; Shetty, P. P.; Kondekar, N.; Wang, C.; Li, W.; McDowell, M. T. Enabling Highly Reversible Sodium Metal Cycling across a Wide Temperature Range with Dual-Salt Electrolytes. *J. Mater. Chem. A* **2021**, *9* (17), 10992–11000. https://doi.org/10.1039/d1ta00842k.

(35) Wang, B.; Huang, Y.; Wang, Y.; Wang, H. Synergistic Solvation of Anion: An Effective Strategy toward Economical High-Performance Dual-Ion Battery. *Adv. Funct. Mater.* **2023**. https://doi.org/10.1002/adfm.202212287.

(36) Feng, T.; Yang, G.; Zhang, S.; Xu, Z.; Zhou, H.; Wu, M. Low-Temperature and High-Voltage Lithium-Ion Battery Enabled by Localized High-Concentration Carboxylate Electrolytes. *Chem. Eng. J.* **2022**, *433* (P1), 134138. https://doi.org/10.1016/j.cej.2021.134138.

(37) Lin, Z.; Xia, Q.; Wang, W.; Li, W.; Chou, S. Recent Research Progresses in Ether- and Ester-Based Electrolytes for Sodium-Ion Batteries. *InfoMat* **2019**, *1* (3), 376–389. https://doi.org/10.1002/inf2.12023.

(38) Watanabe, Y.; Kinoshita, S. ichi; Wada, S.; Hoshino, K.; Morimoto, H.; Tobishima, S. ichi. Electrochemical Properties and Lithium Ion Solvation Behavior of Sulfone-Ester Mixed Electrolytes for High-Voltage Rechargeable Lithium Cells. *J. Power Sources* **2008**, *179* (2), 770–779. https://doi.org/10.1016/j.jpowsour.2008.01.006.

(39) Petibon, R.; Harlow, J.; Le, D. B.; Dahn, J. R. The Use of Ethyl Acetate and Methyl Propanoate in Combination with Vinylene Carbonate as Ethylene Carbonate-Free Solvent Blends for Electrolytes in Li-Ion Batteries. *Electrochim. Acta* **2015**, *154*, 227–234. https://doi.org/10.1016/j.electacta.2014.12.084.

(40) Hall, D. S.; Eldesoky, A.; Logan, E. R.; Tonita, E. M.; Ma, X.; Dahn, J. R. Exploring Classes of Co-Solvents for Fast-Charging Lithium-Ion Cells. *J. Electrochem. Soc.* **2018**, *165* (10), A2365–A2373. https://doi.org/10.1149/2.1351810jes.

(41) Chemical Properties of Propanoic acid, ethyl ester (CAS 105-37-3) https://www.chemeo.com/cid/15-398-4/Propanoic-acid-ethyl-ester.

(42) Chemical Properties of Methyl isobutyrate (CAS 547-63-7) https://www.chemeo.com/cid/45-945-3/Methyl-isobutyrate.

(43) Seo, D. M.; Reininger, S.; Kutcher, M.; Redmond, K.; Euler, W. B.; Lucht, B. L. Role of Mixed Solvation and Ion Pairing in the Solution Structure of Lithium Ion Battery Electrolytes. *J. Phys. Chem. C* **2015**, *119* (25), 14038–14046. https://doi.org/10.1021/acs.jpcc.5b03694.

(44) Chua, S. C.; Chong, F. K.; Ul Mustafa, M. R.; Mohamed Kutty, S. R.; Sujarwo, W.; Abdul Malek, M.; Show, P. L.; Ho, Y. C. Microwave Radiation-Induced Grafting of 2-Methacryloyloxyethyl Trimethyl Ammonium Chloride onto Lentil Extract (LE-g-DMC) as an Emerging High-Performance Plant-Based Grafted Coagulant. *Sci. Rep.* **2020**, *10* (1), 1–

13. https://doi.org/10.1038/s41598-020-60119-x.